

# Polarization degrees of freedom in near-threshold photoproduction of $\omega$ mesons in the $\pi^0\gamma$ decay channel

A.V. Sarantsev<sup>1,2</sup>, A.V. Anisovich<sup>1,2</sup>, V.A. Nikonov<sup>1,2</sup> and H. Schmieden<sup>3</sup>

<sup>1</sup> Helmholtz-Institut für Strahlen- und Kernphysik, Universität Bonn, Germany

<sup>2</sup> Petersburg Nuclear Physics Institute, Gatchina, Russia

<sup>3</sup> Physikalisches Institut, Universität Bonn, Germany

November 12, 2018

**Abstract.** We study polarization variables in the photoproduction of  $\omega$ -mesons with subsequent  $\omega \rightarrow \gamma\pi^0$  decay. Single and double polarization observables are calculated as a function of different final-state angles. Reaction models include pomeron (natural parity) and  $\pi^0$  (unnatural parity) exchange in the  $t$ -channel. In addition, the contribution of  $s$ -channel resonances is considered. The sensitivity of the polarization observables to the reaction dynamics is discussed.

**PACS.** 11.80.Et Partial-wave analysis – 13.30.-a Decays of baryons – 13.60.Le Meson production

## 1 Introduction

The hadron mass spectrum and hadronic decay modes provide important information towards the understanding of strong interactions at low and intermediate energies. While in the meson sector the number of observed states roughly corresponds to the prediction of the quark model, in the baryon sector the expected spectrum of such models [1, 2, 3, 4] is much richer than observed [5]. The possibility is discussed that the *missing resonances* may have escaped observation in pion induced processes due to their small  $N\pi$  coupling [2, 6, 7]. The *photoproduction* of mesons offers a means to get a hand on the existence of the missing states, in particular in non-pionic final states.

The photoproduction of  $\omega$  mesons off the proton is well suited to investigate this issue. It benefits from the fact that the  $\omega$  threshold is in the higher lying third resonance region of the nucleon. The narrow width of 8 MeV enables a clean detection of the  $\omega$  over background. In addition, the  $\omega$  is isoscalar ( $I = 0$ ); hence a  $s$ -channel process will only connect  $N^*$  ( $I = 1/2$ ) states with the nucleon ground state, but no  $\Delta^*$  with  $I = 3/2$ . This provides a great simplification to the complexity of the contributing excitation spectrum.

Several recent experiments [8, 9, 10] and coupled channel analyses [11, 12] reported evidence for resonance contributions close to  $\omega$  production threshold. Usually the  $\omega$  is detected through the charged decay  $\omega \rightarrow \pi^+\pi^-\pi^0$ . The neutral  $\omega \rightarrow \pi^0\gamma$  decay provides complementary information [13]. Recently, first beam asymmetries have been measured using this channel [14].

In order to disentangle the reaction mechanism and characterize individual resonance contributions, the measurement of polarization observables is indispensable. A completely unambiguous decomposition of the reaction amplitudes would require at least 23 independent observables to be measured, including double and triple polarization observables.

It is the scope of the present paper to investigate single and double polarization observables in the reaction  $\gamma p \rightarrow \omega p \rightarrow \pi^0\gamma p$ . The sensitivity of the observables to resonance contributions to  $\omega$  photoproduction is investigated.

The paper is organized as follows. Cross section and polarization observables are first discussed on the basis of the reaction dynamics. The influence of the reaction mechanism on the observables is then investigated in section 3, in particular the sensitivity to  $s$ -channel resonance contributions. The main results are finally summarized.

## 2 Cross sections, angular distributions and polarization variables

The differential cross section for production of two or more particles has the general form

$$d\sigma = \frac{(2\pi)^4 |A|^2}{4\sqrt{(k_1 k_2)^2 - m_1^2 m_2^2}} d\Phi_n(k_1 + k_2, q_1, \dots, q_n) \quad (1)$$

where  $k_1$  and  $k_2$  are the momenta of the initial particles  $k_i^2 = m_i^2$  (nucleon and  $\gamma$  in the case of photoproduction) and  $q_i$  denote the momenta of the final state particles.

$d\Phi_n$  is the  $n$ -body phase volume given by

$$d\Phi_n(k_1 + k_2, q_1, \dots, q_n) = \delta^4(k_1 + k_2 - \sum_{i=1}^n q_i) \prod_{i=1}^n \frac{d^3 q_i}{(2\pi)^3 2q_{0i}}. \quad (2)$$

The amplitude for photoproduction of a single (pseudo-) scalar meson is written in the form

$$A = \varepsilon_\mu \bar{u}(q_1) A_\mu u(k_1), \quad (3)$$

where  $\varepsilon_\mu$  is the photon polarization vector and  $\bar{u}(q_1)$  and  $u(k_1)$  are bispinors of the final and initial nucleons with momenta  $q_1$  and  $k_1$ , respectively. When the polarizations of photon and nucleon are not measured the squared amplitudes are averaged over orthogonal polarization vectors of the initial particles and summed over polarization vectors of the final particles:

$$|A|^2 = \frac{1}{4} \sum_{\alpha ij} \varepsilon_\mu^\alpha \varepsilon_\nu^{\alpha*} \bar{u}^i(q_1) A_\mu u^j(k_1) \bar{u}^j(k_1) A_\nu^{tr} u^i(q_1), \quad (4)$$

Here  $A^{tr}$  is the hermitian conjugated amplitude. The index  $\alpha$  describes orthogonal polarization vectors of the photon and  $i, j$  describe the two orthogonal polarizations of the initial and final bispinors.

The amplitude for the photoproduction of vector mesons has the structure

$$A = \varepsilon_\mu \bar{u}(q_1) A_{\mu\nu} u(k_1) \omega_\nu, \quad (5)$$

where  $\omega_\nu$  is the vector-meson polarization vector. The squared amplitude for the unpolarized case is given by

$$|A|^2 = \sum_{\alpha ij} \frac{\varepsilon_\mu^\alpha \varepsilon_\nu^{\alpha*}}{4} \bar{u}^i(q_1) A_{\mu\tau} u^j(k_1) \bar{u}^j(k_1) A_{\nu\xi}^{tr} u^i(q_1) \omega_\tau \omega_\xi^*, \quad (6)$$

For the  $\omega$  meson decaying into three pions, the direction of the  $\omega$  polarization vector is defined by

$$\omega_\xi = \varepsilon_{\xi\alpha\beta\gamma} q_{2\alpha} q_{3\beta} q_{4\gamma} \quad (7)$$

where  $\varepsilon_{\nu\alpha\beta\gamma}$  is the totally antisymmetrical tensor and  $q_i$  are the momenta of the final-state pions. For the  $\pi^0\gamma$  decay, the  $\omega$  polarization vector can be written as

$$\omega_\xi = \frac{1}{M_\omega} \varepsilon_{\xi\alpha\beta\nu} q_\alpha p_\beta \tilde{\epsilon}_\nu \equiv \frac{1}{M_\omega} \varepsilon_{\xi qp\nu} \tilde{\epsilon}_\nu \quad (8)$$

where  $\tilde{\epsilon}_\nu$  is the polarization vector of the final photon,  $q$  is the pion 4-vector ( $q \equiv q_2$ ) and  $p$  is the 4-vector of the  $\omega$ -meson ( $p = q_2 + q_3$  where  $q_3$  is the photon 4-vector). The factor  $1/M_\omega$  ( $M_\omega^2 \equiv p^2$ ) is introduced to avoid the divergence of the amplitude at large energies.

If the polarization of the final photon is not measured, the omega polarization vector can not be completely determined. However its direction should be orthogonal to the plane which is defined by the 4-vectors of the  $\omega$  and  $\pi$  mesons. The product of the  $\omega$  polarization vectors summed over the polarizations of the final photons yields:

$$\omega_\tau \omega_\xi^* = -\frac{1}{M_\omega^2} \varepsilon_{\tau\mu qp} \varepsilon_{\xi\nu qp} \tilde{g}_{\mu\nu}^{\perp\perp} \quad (9)$$

Here  $\tilde{g}_{\mu\nu}^{\perp\perp}$  is a tensor orthogonal to the momentum of the photon (as any photon polarization vector) and to the momentum of one of the another on-shell-particle in the vertex (gauge invariance):

$$-\sum_\alpha \tilde{\varepsilon}_\mu^\alpha \tilde{\varepsilon}_\nu^{\alpha*} = \tilde{g}_{\mu\nu}^{\perp\perp} = g_{\mu\nu} - \frac{p_\mu p_\nu}{M_\omega^2} - \frac{q_\mu^\perp q_\nu^\perp}{q_\perp^2}. \quad (10)$$

where

$$q_\mu^\perp = q_\nu \tilde{g}_{\mu\nu}^{\perp\perp}, \quad \tilde{g}_{\mu\nu}^{\perp\perp} = \left( g_{\mu\nu} - \frac{p_\mu p_\nu}{M_\omega^2} \right). \quad (11)$$

and  $q_\perp^2 = q_\mu^\perp q_\mu^\perp$ . The tensor  $\omega_\tau \omega_\xi^*$ , defined in eq.(9), has the same structure as the tensor  $\tilde{g}_{\mu\nu}^{\perp\perp}$ :

$$\omega_\tau \omega_\xi^* = -(q_\perp^2 \tilde{g}_{\tau\xi}^{\perp\perp} - q_\tau^\perp q_\xi^\perp) \quad (12)$$

For unpolarized photons the product of polarization vectors summed over polarizations gives:

$$-\sum_\alpha \varepsilon_\mu^\alpha \varepsilon_\nu^{\alpha*} = g_{\mu\nu}^{\perp\perp} = g_{\mu\nu} - \frac{P_\mu P_\nu}{P^2} - \frac{k_\mu^\perp k_\nu^\perp}{k_\perp^2} \quad (13)$$

where  $P = k_1 + k_2$  is the total momentum of the  $\gamma N$  system,  $k_1$  is the momentum of the initial nucleon and  $k_2$  is the photon momentum. Then

$$k_\mu^\perp = \frac{1}{2} (k_1 - k_2)_\nu g_{\mu\nu}^{\perp\perp} = \frac{1}{2} (k_1 - k_2)_\nu \left( g_{\mu\nu} - \frac{P_\mu P_\nu}{P^2} \right). \quad (14)$$

In the center-of-mass of the  $\gamma N$  reaction and with the photon momentum directed along the  $z$ -axis the tensor  $g_{\mu\nu}^{\perp\perp}$  has the form:

$$g_{\mu\nu}^{\perp\perp} = \begin{pmatrix} 0 & 0 & 0 & 0 \\ 0 & -1 & 0 & 0 \\ 0 & 0 & -1 & 0 \\ 0 & 0 & 0 & 0 \end{pmatrix}. \quad (15)$$

The bispinors of fermions with momentum  $k_1$  summed over polarizations are:

$$\sum_j u^j(k_1) \bar{u}^j(k_1) = m + \hat{k}_1, \quad \hat{k}_1 \equiv k_{1\mu} \gamma_\mu \quad (16)$$

and therefore the squared amplitude (6) can be rewritten as:

$$|A|^2 = \frac{1}{4} g_{\mu\nu}^{\perp\perp} Tr \left[ (m + \hat{k}_1) A_{\mu\tau} (m + \hat{q}_1) A_{\nu\xi}^{tr} \right] \times (q_\perp^2 \tilde{g}_{\tau\xi}^{\perp\perp} - q_\tau^\perp q_\xi^\perp). \quad (17)$$

It is stressed that the tensor  $g_{\mu\nu}^{\perp\perp}$  is orthogonal to the total momentum of the  $\gamma N$  system, while  $\tilde{g}_{\tau\xi}^{\perp\perp}$  and  $q_\xi^\perp$  are orthogonal to the momentum of the  $\omega$ -meson.

## 2.1 Photon polarizations

When the initial photon is linearly polarized along the  $y$ -axis, the polarization vector in the laboratory and c.m. system is  $\varepsilon_\mu = (0, 0, 1, 0)$  and we do not need to average over the polarizations. In eq.(17) then

$$\frac{1}{2}g_{\mu\nu}^{\perp\perp} \rightarrow \begin{pmatrix} 0 & 0 & 0 & 0 \\ 0 & 0 & 0 & 0 \\ 0 & 0 & -1 & 0 \\ 0 & 0 & 0 & 0 \end{pmatrix} \quad (18)$$

For a circularly polarized beam with helicity  $\pm 1$ ,  $\varepsilon_\mu = \mp \frac{1}{\sqrt{2}}(0, 1, \pm i, 0)$ . For helicity  $+1$  the density matrix is

$$\frac{1}{2}g_{\mu\nu}^{\perp\perp} \rightarrow \frac{1}{2} \begin{pmatrix} 0 & 0 & 0 & 0 \\ 0 & -1 & -i & 0 \\ 0 & i & -1 & 0 \\ 0 & 0 & 0 & 0 \end{pmatrix}. \quad (19)$$

Helicity  $-1$  differs in the sign of the nondiagonal elements.

The photon beam is assumed to have either linear or circular polarization. In general, the degree of polarization is not 100%. Linear polarization is in the range  $0 < P_-^\gamma < +1$ ; the degree of circular polarization  $P_\odot^\gamma$  is between  $-1 < P_\odot^\gamma < +1$ .

## 2.2 Polarized target and recoil polarization

For a polarized target, the density matrix of the nucleon propagator ( $m + \hat{k}_1$ ) must be changed to a polarization density matrix:

$$m + \hat{k}_1 \rightarrow (m + \hat{k}_1)(1 + \gamma_5 \hat{P}^t). \quad (20)$$

where the 4-vector  $P^t$  is the polarization vector of the target baryon. Assuming 100% polarization:

$$P^t = (P_0^t; \mathbf{P}^t) \quad (P^t)^2 = -1, \quad k_1 \cdot P^t = 0. \quad (21)$$

If the baryon momentum is directed along the  $z$  axis

$$k_1 = (\sqrt{m_p^2 + k_z^2}, 0, 0, k_z), \quad (22)$$

then the longitudinal polarization vector is equal to:

$$P^t = \left( \frac{k_z}{m_p}; 0, 0, \frac{\sqrt{m_p^2 + k_z^2}}{m_p} \right). \quad (23)$$

The transverse polarization the polarization vector has only  $x$  and/or  $y$  components.

If the polarization  $P^r$  of the final-state baryon  $P^r = (P_0^r, \mathbf{P}^r)$  is measured, the density matrix of the propagator ( $m + \hat{q}_1$ ) is substituted by

$$m + \hat{q}_1 \rightarrow (m + \hat{q}_1)(1 + \gamma_5 \hat{P}^r), \quad (24)$$

$P^r$  satisfies  $(P^r)^2 = -1$ ,  $q_1 \cdot P^r = 0$ .

## 2.3 Polarization variables for pseudoscalar meson photoproduction

For single pseudoscalar meson photoproduction the description follows a paper by Chiang, Yang, Tiator and Drechsel [15]. The polarized and unpolarized differential cross sections (which we define for the sake of simplicity as  $\sigma \equiv d\sigma/d\Omega$  and  $\sigma_0 \equiv d\sigma_0/d\Omega$ ) can be divided into three classes of double polarization experiments:

– **polarized photons and polarized target**

$$\sigma = \sigma_0 [1 - P_-^\gamma \Sigma \cos 2\Phi + P_x^t (-P_-^\gamma H \sin 2\Phi + P_\odot^\gamma F) - P_y^t (-T + P_-^\gamma P \cos 2\Phi) - P_z^t (-P_-^\gamma G \sin 2\Phi - P_\odot^\gamma E)] \quad (25)$$

which reduces to

$$\sigma = \sigma_0 \{ 1 + P_\odot^\gamma P_z^t E - P_-^\gamma \Sigma \cos 2\Phi + P_-^\gamma P_z^t G \sin 2\Phi \} \quad (26)$$

for target polarization  $\mathbf{P}^t = (0, 0, P_z^t)$  in beam direction. Here we changed the sign of  $E$  polarization compared to [15] to be in correspondence with other analyses (e.g. [16]).

– **polarized photons and recoil polarization**

$$\sigma = \sigma_0 [1 - P_-^\gamma \Sigma \cos 2\Phi + P_x^r (-P_-^\gamma O_{x'} \sin 2\Phi - P_\odot^\gamma C_{x'}) - P_y^r (-P + P_-^\gamma T \cos 2\Phi) - P_z^r (P_-^\gamma O_{z'} \sin 2\Phi + P_\odot^\gamma C_{z'})] \quad (27)$$

– **polarized target and recoil polarization**

$$\sigma = \sigma_0 [1 + P_y^r P + P_x^t (P_x^r T_{x'} + P_z^r T_{z'}) + P_y^t (T + P_y^r \Sigma) - P_z^t (P_x^r L_{x'} - P_z^r L_{z'})] \quad (28)$$

In all cases  $\Phi$  denotes the angle between the photon polarization vector and the reaction plane ( $xz$ ) (see Fig.1). The polarization of the recoil baryon is measured in a coordinate system ( $x', y', z'$ ) where  $z'$  is defined by the direction of the recoil baryon,  $y' = y$  and  $x'$  is orthogonal to  $y', z'$ .

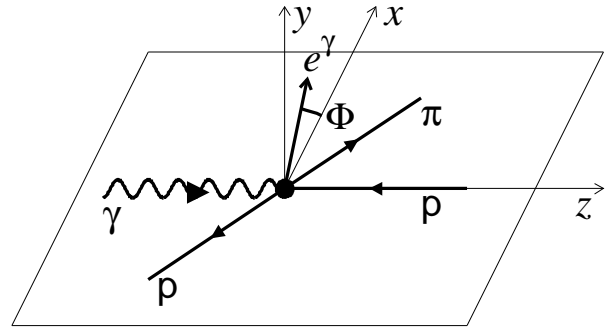


**Fig. 1.** The definition of the  $\Phi$  angle for the single-pion photoproduction, (from [15])

## 2.4 Coordinate frame fixed by the polarization of initial particles

In most papers devoted to polarization variables the amplitude is calculated in the frame where the  $x$ -axis together with the  $z$ -axis forms the reaction plane. The azimuthal angle  $\Phi$  is defined as the angle between the reaction plane and the direction of photon polarization. For double polarization observables, e.g. beam-transverse target, the calculations are made with target polarization directed along one of the axes in this coordinate frame. Experimentally, the angle between beam and transverse target polarization is fixed and it may be advantageous to fix the axes by these polarizations. To extract the dependence of the cross section on the azimuthal angle in such a frame, eq. (25) must be rotated by  $\varphi$  which is angle between the  $x$  axis and the direction of the meson momentum. For unpolarized photons, in the frame where target polarization (100%) is directed along  $y$ -axis:

$$\sigma = \sigma_0 [1 + T \cos \varphi] \quad (29)$$

The definition of the angles is shown in Fig.2.

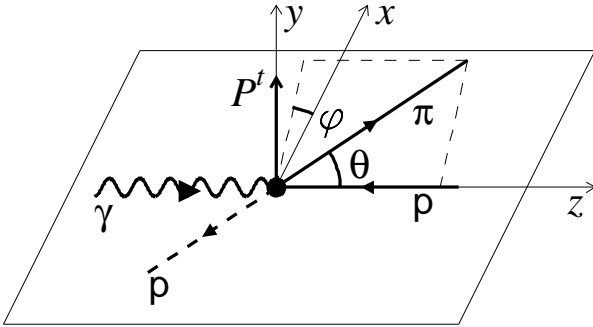


**Fig. 2.** The definition of the  $\varphi$  angle for the single pion photoproduction with the target polarization directed along the  $y$ -axis

Let us list here the final expressions for the beam target polarization experiment. If the target polarization is directed along the  $y$ -axis then one obtains for the beam polarizations directed along  $x$  ( $\sigma_x^y$ ),  $y$  ( $\sigma_y^y$ ), and for unpolarized beam ( $\sigma_0^y$ ):

$$\begin{aligned} \frac{\sigma_x^y}{\sigma_0} &= 1 - \Sigma \cos 2\varphi + \left(T - \frac{H+P}{2}\right) \cos \varphi + \frac{H-P}{2} \cos 3\varphi \\ \frac{\sigma_y^y}{\sigma_0} &= 1 + \Sigma \cos 2\varphi + \left(T + \frac{H+P}{2}\right) \cos \varphi - \frac{H-P}{2} \cos 3\varphi \\ \frac{\sigma_0^y}{\sigma_0} &= 1 + T \cos \varphi. \end{aligned} \quad (30)$$

If the photon polarization is directed along the  $x$  axis  $\varphi = \Phi$  from eqs.(25) and if it is directed along the  $y$  axis  $\varphi = 90^\circ - \Phi$ .

With one receives circular polarized beam with helicity +1:

$$\frac{\sigma_{\odot}^y}{\sigma_0} = 1 + T \cos \varphi + F \sin \varphi. \quad (31)$$

If the target polarization is directed along  $x$ -axis we have

$$\begin{aligned} \frac{\sigma_x^x}{\sigma_0} &= 1 - \Sigma \cos 2\varphi - \left(T + \frac{H+P}{2}\right) \sin \varphi - \frac{H-P}{2} \sin 3\varphi \\ \frac{\sigma_y^x}{\sigma_0} &= 1 + \Sigma \cos 2\varphi - \left(T - \frac{H+P}{2}\right) \sin \varphi + \frac{H-P}{2} \sin 3\varphi \\ \frac{\sigma_0^x}{\sigma_0} &= 1 - T \sin \varphi, \end{aligned} \quad (32)$$

and with circular polarization (helicity +1):

$$\frac{\sigma_{\odot}^x}{\sigma_0} = 1 - T \sin \varphi + F \cos \varphi \quad (33)$$

For a photon polarization directed at 45 degrees relative to the  $x$ -axis

$$\begin{aligned} \frac{\sigma_{45}^0}{\sigma_0} &= 1 - \Sigma \sin 2\varphi - T \sin \varphi \\ &\quad + \frac{H+P}{2} \cos \varphi + \frac{H-P}{2} \cos 3\varphi \end{aligned} \quad (34)$$

is obtained. In all expressions a 100% beam and target polarization is assumed.

It is seen that the extraction of the polarization variables is a difficult task: e.g. if the target polarization is directed along the  $y$ -axis and the beam polarization along the  $x$ -axis, the polarized cross section should be first to be decomposed into three  $\varphi$  dependencies which provide the beam asymmetry and two combinations of  $T$ ,  $H$  and  $P$  observables. Due to orthogonality condition

$$\begin{aligned} \int_0^{2\pi} \cos(n\varphi) \frac{d\varphi}{2\pi} &= \int_0^{2\pi} \sin(n\varphi) \frac{d\varphi}{2\pi} = 0 \\ \int_0^{2\pi} \cos^2(n\varphi) \frac{d\varphi}{2\pi} &= \int_0^{2\pi} \sin^2(n\varphi) \frac{d\varphi}{2\pi} = \frac{1}{2} \end{aligned} \quad (35)$$

for any  $n = 1, 2, 3, \dots$ , the  $T - (H + P)/2$  combination can be extracted directly from the polarization data by weighting the events with  $\cos \varphi$ :

$$T - \frac{H+P}{2} = \frac{2}{\sigma_0} \int_0^{2\pi} \sigma_x^y \cos \varphi \frac{d\varphi}{2\pi} \quad (36)$$

Such variable can also be directly compared with theoretical prediction.

## 2.5 Two pseudoscalar meson photoproduction

For the photoproduction of two mesons the number of polarization variables is much larger. Already in the case of

polarized beam and unpolarized target a beam asymmetry can be extracted for every outgoing particle. Moreover, the polarization observables can be extracted from the  $\varphi$  dependencies calculated in the center-of-mass system of two final particles. There are also new observables compared to single meson photoproduction. For example, in the case of the single meson photoproduction the circular polarization of the beam does not provide any additional information if the target is unpolarized and the polarization of the final proton is not measured. However in two meson photoproduction the circular polarization alone can effectively provide a beam-recoil asymmetry: for example in the case of  $\Delta\pi$  final state some information about  $\Delta$  polarization can be obtained from its decay into  $\pi N$ .

## 2.6 Vector meson photoproduction

Polarization variables have been extensively studied in  $\omega$  photoproduction for the case of the linear polarized beam and unpolarized target and, in particular, for the  $\omega$  meson decaying into three pions, e.g [17, 18, 19]. For linear (or circular) polarized beam and polarized target, and radiative omega decay into  $\pi^0\gamma$  the theory is not fully developed. In the present paper we concentrate on polarization observables in the photoproduction of  $\omega$  mesons with subsequent decays  $\omega \rightarrow \pi^0\gamma$ . The formalism is the same for the radiative  $\Phi$  decays into  $\eta\gamma$  (with a branching ratio of  $BR = 1.3\%$ ) and  $\pi^0\gamma$  ( $BR = 0.13\%$ ).

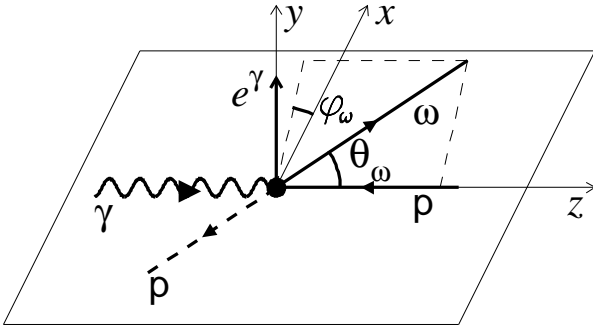


**Fig. 3.** The definition of the  $\varphi_\omega$  angle for the  $\omega$ -meson photoproduction with the beam polarization directed along the  $y$ -axis

The  $z$ -axis is usually chosen along the initial beam. For unpolarized single pseudoscalar-meson photoproduction there is no additional vector to fix the azimuthal angle. It is a 'one-plane' reaction and the measured cross section should not depend how this plane is oriented. In the case of unpolarized vector meson photoproduction the situation is more complicated: if the polarization of the  $\omega$  is, at least partly, measured, then there are two planes involved and dependencies on the relative azimuthal angle of the  $\omega$  and  $\pi^0$  can be obtained. This is similar to the situation with two pseudoscalar mesons in the final state.

With linearly polarized beam the cross section should not change, if the photon polarization vector is rotated by 180 degrees and, therefore, the beam polarization enters with a  $2n\varphi$  dependence. In  $\omega$  photoproduction three beam asymmetries can be naturally extracted: the beam asymmetry of the  $\omega$  meson calculated in the c.m.s. of the reaction,  $\Sigma$  (omega asymmetry), the beam asymmetry of the final pion in the c.m.s. of the reaction,  $\Sigma_\pi$  (pion asymmetry), and the beam asymmetry of the final pion in the rest frame of the  $\omega$ ,  $\Sigma_\pi^\omega$  (pion-in-omega-rest-frame asymmetry). The decay asymmetry  $\Sigma_d$  introduced for the decay of vector mesons into two and three pseudoscalar particles (see e.g. [17, 20, 21]) is extracted as a coefficient in front of the  $\cos 2\Psi$  dependence in the production cross section, where  $\Psi$  is the angle between the photon polarization and the momentum of the final pseudoscalar meson. If this definition is extended to  $\omega$ 's decaying into  $\pi^0\gamma$ , the decay asymmetry differs by a sign from  $\Sigma_\pi^\omega$ :

$$\Sigma_d = -\Sigma_\pi^\omega. \quad (37)$$

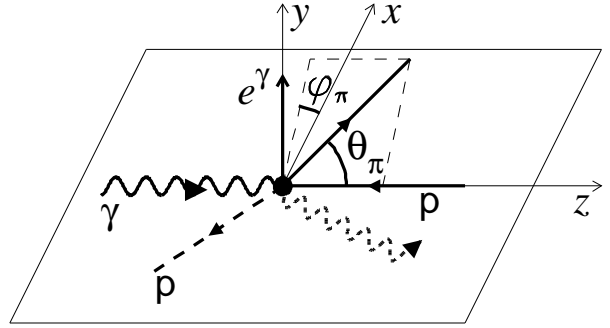


**Fig. 4.** The definition of the  $\varphi_\pi$  angle for the  $\omega$ -meson photoproduction with the beam polarization directed along the  $y$ -axis

By means of the orthogonality condition (35) the asymmetries can be defined from the cross section obtained with a photon beam polarized linearly along the  $y$ -axis as:

$$\begin{aligned} \Sigma &= \frac{2}{\sigma_0} \int_0^{2\pi} \sigma_y \cos 2\varphi_\omega \frac{d\varphi_\omega}{2\pi}, & \Sigma_\pi &= \frac{2}{\sigma_0} \int_0^{2\pi} \sigma_y \cos 2\varphi_\pi \frac{d\varphi_\pi}{2\pi}, \\ \Sigma_\pi^\omega &= \frac{2}{\sigma_0} \int_0^{2\pi} \sigma_y \cos 2\varphi_\pi^\omega \frac{d\varphi_\pi^\omega}{2\pi}. \end{aligned} \quad (38)$$

The definition of the  $\varphi_\omega$  and  $\varphi_\pi$  angles are shown in Figs. 3,4. The beam asymmetries can be extracted directly from the experimental data through their specific  $\varphi$  dependence.

This also holds for the beam-target double polarization observables, e.g of G-type. The  $G$ ,  $G_\pi$ ,  $G_\pi^\omega$  observables can be calculated from the polarized cross section obtained

with linear polarized beam (e.g. along the  $y$ -axis) and target polarization along the  $z$ -axis. These variables have a  $\sin 2\varphi$  dependence:

$$G = \frac{2}{\sigma_0} \int_0^{2\pi} \sigma_y \sin 2\varphi_\omega \frac{d\varphi_\omega}{2\pi}, \quad G_\pi = \frac{2}{\sigma_0} \int_0^{2\pi} \sigma_y \sin 2\varphi_\pi \frac{d\varphi_\pi}{2\pi},$$

$$G_\pi^\omega = \frac{2}{\sigma_0} \int_0^{2\pi} \sigma_y \sin 2\varphi_\pi \frac{d\varphi_\pi^\omega}{2\pi} \quad (39)$$

The observable  $E$  is the asymmetry of helicity  $3/2$  and  $1/2$  initial states,

$$E = \frac{\sigma_{3/2} - \sigma_{1/2}}{\sigma_{3/2} + \sigma_{1/2}}. \quad (40)$$

It is measured using circular polarized beam and longitudinal polarized target. There is no dependence on any  $\varphi$  angle additional to the unpolarized case.

### 3 Sensitivity of the polarization variables to the vectormeson production dynamics

The main contribution to the  $\gamma p \rightarrow \omega p$  cross section at photon energies above 3 GeV comes from the fluctuation of the photon into a vector meson. In this regime the cross section exhibits diffractive behavior [22, 21, 23, 24] and has an exponential  $t$ -dependence

$$\frac{d\sigma}{dt} \simeq \left. \frac{d\sigma}{dt} \right|_{t=0} \cdot e^{-b|t|}, \quad (41)$$

where the parameter  $|b|$  characterizes the range of the vector-meson-nucleon interaction. The photon helicity is transferred to the vector meson, i.e. the  $s$ -channel helicity is conserved. This requires  $(-)^J$  natural parity of the exchange particle, i.e.  $0^+$ ,  $1^-$ , etc. (“Pomeron”), and intricate conspiracy between  $t$ -channel spin-flip and non spin-flip contributions [25]. At energies below 3 GeV both exchange-parity characteristics are expected to contribute on a similar level. The unnatural parity admixture is attributed to  $t$ -channel exchange of pseudoscalar mesons, in particular  $\pi^0$  [26]. Resonances in the  $s$ -channel are preferably expected to show up in the threshold region, since they would be form-factor suppressed at higher energies.

Polarization observables have been extensively studied in  $\omega$  photoproduction for the case of linear polarized beam and unpolarized target and, in particular, for the  $\omega$  decaying into three pions (see e.g. [17]). For forthcoming experiments with linearly or circularly polarized beam and polarized target which use the radiative  $\omega$  decay the theory is not fully developed. In the following we examine characteristic signatures of the different pieces of the reaction mechanism on the polarization observables in the reaction  $\gamma p \rightarrow \omega p \rightarrow \gamma \pi^0 p$ .

#### 3.1 Pion exchange

The  $\omega$  meson decays in a P-wave into the  $\pi^0 \gamma$  system. The amplitude is described by the convolution of the antisymmetrical tensor with the momentum of the photon, the momentum of the  $\omega$ -meson and the polarization vectors of omega and photon.

In the case of a pion exchange in the  $t$ -channel the omega production is described by the amplitude

$$\tilde{A}_{\gamma p \rightarrow \omega p}^{ij} = A_{\pi^*}^{ij} A(p \rightarrow \pi^* p), \quad \text{where}$$

$$A_{\pi^*}^{ij} = \epsilon_\mu^{(i)} \varepsilon_{\mu\alpha kp} \omega_\alpha = \epsilon_\mu^{(i)} \varepsilon_{\mu\alpha kp} \frac{1}{M_\omega} \varepsilon_{\nu\alpha qp} \tilde{\epsilon}_\nu^{(j)}. \quad (42)$$

Here  $k$  is the momentum of the initial photon ( $k \equiv k_2$ ),  $q$  the momentum of the final pion ( $q \equiv q_2$ ),  $p$  the momentum of the  $\omega$ -meson and

$$\varepsilon_{\mu\alpha qp} \equiv \varepsilon_{\mu\alpha\nu\mu} q_\mu p_\nu. \quad (43)$$

The  $\epsilon_\mu^{(i)}$  and  $\tilde{\epsilon}_\nu^{(j)}$  are the polarization vectors of the initial and final photon, respectively. The amplitude  $A(p \rightarrow \pi^* p)$  describes the propagation of the virtual pion ( $\pi^*$ ) and its absorption by the proton.

The unpolarized cross section is proportional to the squared amplitude summed over the polarization of the final photon and nucleon, and averaged over the polarization of the initial photon and nucleon:

$$\sigma_0 = \frac{1}{4} \sum_{i,j=1}^2 |A_{\pi^*}^{ij}|^2 \frac{(2\pi)^4 |A(p \rightarrow \pi^* p)|^2}{4\sqrt{(k_1 k_2)^2 - m_1^2 m_2^2}} d\Phi_n \quad (44)$$

where  $d\Phi_n$  is defined by eq.(2). The amplitude for the interaction of the virtual pion with the nucleon can be factorized out from the production of the  $\omega$ -meson.

We first consider the beam asymmetry in the rest frame of the omega meson. If the  $z$ -axis is directed along the beam, then:

$$q = (q_0; |\mathbf{q}| \sin \Theta_\pi \cos \varphi_\pi, |\mathbf{q}| \sin \Theta_\pi \sin \varphi_\pi, |\mathbf{q}| \cos \Theta_\pi)$$

$$p = (M_\omega; 0, 0, 0) \quad k = (k_0; 0, 0, k_z). \quad (45)$$

The  $y, x$ -axes can be chosen in the way that two orthogonal polarization vectors of the initial photon (which are  $\epsilon^{(y)} = (0; 0, 1, 0)$  and  $\epsilon^{(x)} = (0; 1, 0, 0)$  in c.m.s. of the reaction) have also only one component in the  $xy$  plane in the omega rest frame. The boost of these vectors to the  $\omega$  rest frame yields:

$$\epsilon^{(y)} = \left(-\frac{\omega_y}{M_\omega}; 0, 1, -\frac{\omega_y}{M_\omega}\right),$$

$$\epsilon^{(x)} = \left(-\frac{\omega_x}{M_\omega}; 1, 0, -\frac{\omega_x}{M_\omega}\right) \quad (46)$$

where  $\omega_x$  and  $\omega_y$  are the  $x$  and  $y$ -components of the  $\omega$ -meson momentum in c.m.s. of the reaction:

$$p = (\omega_0; \omega_x, \omega_y, \omega_z) \quad \text{in c.m.s..} \quad (47)$$

Summing over the polarization of the final photons (of eq. (12) we obtain for the squared amplitude:

$$|A^i|^2 = \sum_{j=1}^2 |A^{ij}|^2 = -\epsilon_{\mu}^{(i)} \epsilon_{\nu}^{(j)*} \varepsilon_{\mu\alpha kp} \varepsilon_{\nu\beta kp} \times (q_{\perp}^2 g_{\alpha\beta}^{\perp} - q_{\alpha}^{\perp} q_{\beta}^{\perp}). \quad (48)$$

Due to the fact that the omega 4-momentum has only an energy component and the momentum of the initial photon has only energy and  $z$  components, the antisymmetrical tensor can be written as

$$\varepsilon_{\mu\alpha kp} = \varepsilon_{\mu\alpha z0} k_z M_{\omega}. \quad (49)$$

Therefore only  $y$  and  $x$  components of the polarization vectors of the initial photon give a contribution to the cross section. For the squared amplitude we then obtain:

$$\begin{aligned} |A^y|^2 &= k_z^2 M_{\omega}^2 (|\mathbf{q}|^2 - q_x q_x) \\ |A^x|^2 &= k_z^2 M_{\omega}^2 (|\mathbf{q}|^2 - q_y q_y). \end{aligned} \quad (50)$$

Averaging over the polarization of the initial photon yields

$$\begin{aligned} \frac{|A^x|^2 + |A^y|^2}{2} &= k_z^2 M_{\omega}^2 \left( \mathbf{q}^2 - \frac{q_x q_x + q_y q_y}{2} \right) \\ &= k_z^2 M_{\omega}^2 \frac{\mathbf{q}^2}{2} (1 + z_{\pi}^2), \end{aligned} \quad (51)$$

where  $z_{\pi}^{\omega} \equiv \cos \Theta_{\pi}$  is defined in the rest frame of the  $\omega$ -meson.

If the beam polarization vector is chosen along the  $x$ -axis, then

$$\begin{aligned} |A^x|^2 &= \frac{|A^x|^2 + |A^y|^2}{2} + k_z^2 M_{\omega}^2 \frac{q_x q_x - q_y q_y}{2} = \\ &= \frac{|A^x|^2 + |A^y|^2}{2} + k_z^2 M_{\omega}^2 \frac{|\mathbf{q}|^2}{2} (1 - z_{\pi}^{\omega 2}) \cos 2\varphi_{\pi}^{\omega} \end{aligned} \quad (52)$$

is obtained. Assuming 100% polarization:

$$\sigma_x = \sigma_0 (1 - \Sigma_{\pi}^{\omega} \cos 2\varphi_{\pi}^{\omega}), \quad (53)$$

and we obtain:

$$\Sigma_{\pi}^{\omega} = -\frac{1 - z_{\pi}^{\omega 2}}{1 + z_{\pi}^{\omega 2}}. \quad (54)$$

If the photon polarization is directed along the  $y$  axis

$$\sigma_y = \sigma_0 (1 + \Sigma_{\pi}^{\omega} \cos 2\varphi_{\pi}^{\omega}). \quad (55)$$

There is no dependence of  $\Sigma_{\pi}^{\omega}$  on the other angles, e.g. the angle of the omega in the c.m.s. of the reaction. Thus, integrating the polarized and non-polarized cross section over  $z_{\pi}^{\omega}$  we obtain in the omega rest frame.

$$\Sigma_{\pi}^{\omega} = -\frac{1 - 1/3}{1 + 1/3} = -\frac{1}{2}. \quad (56)$$

In the non-relativistic limit where  $|\omega| < M_{\omega}$  eq.(47) the boost from the  $\omega$  rest frame to the c.m.s. frame does

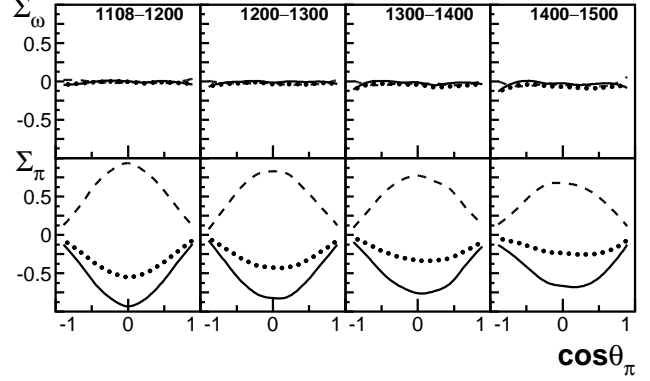


**Fig. 5.** Prediction for the omega asymmetry  $\Sigma_{\omega}$  and the pion asymmetry  $\Sigma_{\pi}$  as a function of the angle between beam and  $\pi$ -meson calculated in the c.m.s. of the reaction in the indicated bins of photon energy between threshold and  $E_{\gamma} = 1500$  MeV. The asymmetry related to pion exchange is shown as solid line, pomeron exchange as dashed line and mixture (see text) of pion and pomeron exchanges as dotted line.

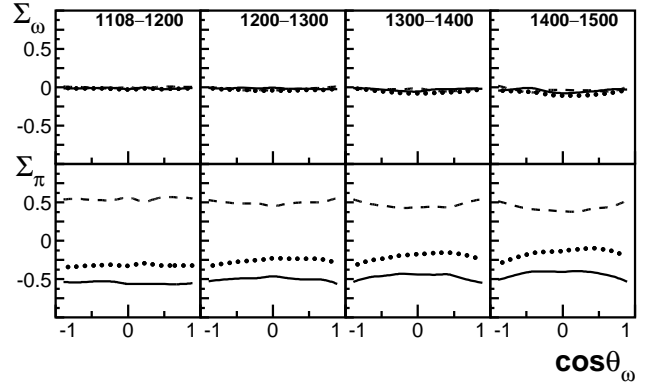


**Fig. 6.** Prediction for the omega asymmetry  $\Sigma_{\omega}$  and the pion asymmetry  $\Sigma_{\pi}$  as a function of the angle between beam and  $\omega$ -meson calculated in the c.m.s. of the reaction. Notation of curves and energy bins is the same as in Fig. 5.

not change the polarization vectors of the photon. This means that the dependence of  $\Sigma_{\pi}$  on the  $z_{\pi}$  (calculated in c.m.s. of the initial photon and proton) should be the same as the dependence of  $\Sigma_{\pi}^{\omega}$  on  $z_{\pi}^{\omega}$  calculated in the rest frame of omega. With increasing energy the boost becomes more important. To extract these variables we performed simulations of  $\Sigma_{\pi}$  and  $\Sigma_{\omega}$  with the Bonn-Gatchina partial wave analysis program. Here the pion exchange amplitude was taken in a reggeized form and the polarized and unpolarized cross sections were calculated from a sample of 400 000  $\gamma p \rightarrow \omega p$  Monte Carlo events. The angular dependence of  $\Sigma_{\pi}$  and  $\Sigma_{\omega}$  on  $z_{\pi}$  at different energies of the initial photon is shown in Fig.5.  $\Sigma_{\pi}$  has the angular dependence close to  $(1 - z_{\pi}^2)/(1 + z_{\pi}^2)$  while the omega asymmetry is equal to zero. Indeed, for pure  $\pi^*$  exchange the cross section measured with linear polarized beam carries no dependence on the azimuthal angle of the  $\omega$ -meson and hence this asymmetry is expected to vanish. The dependence of the  $\Sigma_{\pi}$  and  $\Sigma_{\omega}$  observables on the  $\cos \Theta_{\omega}$  is shown in Fig.6. Both variables show no dependence on this angle

at small energies. Again, as expected, the  $\Sigma_\pi$  asymmetry is close to  $-0.5$  and  $\Sigma_\omega$  is equal to zero. Only at large energies a weak dependence of  $\sigma_\pi$  on  $\cos\Theta_\omega$  is observed.

### 3.2 Pomeron exchange

To investigate the pomeron exchange the leading  $\gamma$ -Pomeron- $\omega$  vertex with S-wave orbital moment between pomeron and initial photon is considered. The omega photoproduction amplitude for such a mechanism has the form:

$$\begin{aligned}\tilde{A}_{\gamma p \rightarrow \omega p}^{ij} &= A_{0+}^{ij} A(p \rightarrow 0^+ p) \\ A_{0+}^{ij} &= \epsilon_\mu^{(i)} \omega_\mu = \epsilon_\mu^{(i)} \frac{1}{M_\omega} \varepsilon_{\nu\mu qp} \tilde{\epsilon}_\nu^{(j)}.\end{aligned}\quad (57)$$

Here  $A(p \rightarrow 0^+ p)$  is the amplitude describing the pomeron propagation and the interaction of the pomeron with the nucleon. Summing over the polarizations of the final photons yields:

$$|A_{0+}^{ij}|^2 = \sum_{j=1}^2 |A_{0+}^{ij}|^2 = -\epsilon_\mu^{(i)} \epsilon_\nu^{(i)*} (q_\perp^2 g_{\mu\nu}^\perp - q_\mu^\perp q_\nu^\perp). \quad (58)$$

Here the z-component of the polarization vector is to be taken into account. Then

$$\begin{aligned}|A_{0+}^y|^2 &= |\mathbf{q}|^2 \left(1 + \frac{w_y^2}{M_\omega^2}\right) - (q_y - q_z \frac{w_y}{M_\omega})^2 \quad \text{and} \\ |A_{0+}^x|^2 &= |\mathbf{q}|^2 \left(1 + \frac{w_x^2}{M_\omega^2}\right) - (q_x - q_z \frac{w_x}{M_\omega})^2\end{aligned}\quad (59)$$

The unpolarized cross section is proportional to:

$$\begin{aligned}\frac{|A^x|^2 + |A^y|^2}{2} &= \frac{|\mathbf{q}|^2}{2} \left(1 + z_\pi^{\omega 2} + \frac{|\mathbf{w}|^2}{M_\omega^2} (1 - z_\pi^{\omega 2}) (1 - z_\omega^2)\right) \\ &+ 2 \frac{z_\pi^\omega |\mathbf{w}|}{M_\omega} \sqrt{(1 - z_\pi^{\omega 2}) (1 - z_\omega^2)} \cos(\varphi_\pi^\omega - \varphi_\omega).\end{aligned}\quad (60)$$

There is a dependence on the difference between the angles  $\varphi_\omega$  and  $\varphi_\pi^\omega$ . This is a consequence of the fact that the polarization vector of the  $\omega$ -meson is partially reconstructed through the  $\gamma\pi$  decay. In a sense we deal with an "incomplete" recoil polarization experiment.

For the initial photon polarization vector along the  $x$ -axis one receives:

$$\begin{aligned}|A^x|^2 &= \frac{|A^x|^2 + |A^y|^2}{2} - \frac{|\mathbf{q}|^2}{2} \left( \cos 2\varphi_\pi^\omega (1 - z_\pi^{\omega 2}) \right. \\ &- \cos 2\varphi_\omega \frac{|\mathbf{w}|^2}{M_\omega^2} (1 - z_\pi^{\omega 2}) (1 - z_\omega^2) \\ &- \left. 2 \frac{z_\pi^\omega |\mathbf{w}|}{M_\omega} \sqrt{(1 - z_\pi^{\omega 2}) (1 - z_\omega^2)} \cos(\varphi_\pi^\omega + \varphi_\omega) \right).\end{aligned}\quad (61)$$

Extracting the  $\cos 2\varphi_\pi^\omega$  dependence only and integrating over all other  $\varphi$  dependencies we obtain

$$\Sigma_\pi^\omega = \frac{1 - z_\pi^{\omega 2}}{1 + z_\pi^{\omega 2} + \frac{|\mathbf{w}|^2}{M_\omega^2} (1 - z_\pi^{\omega 2}) (1 - z_\omega^2)}. \quad (62)$$

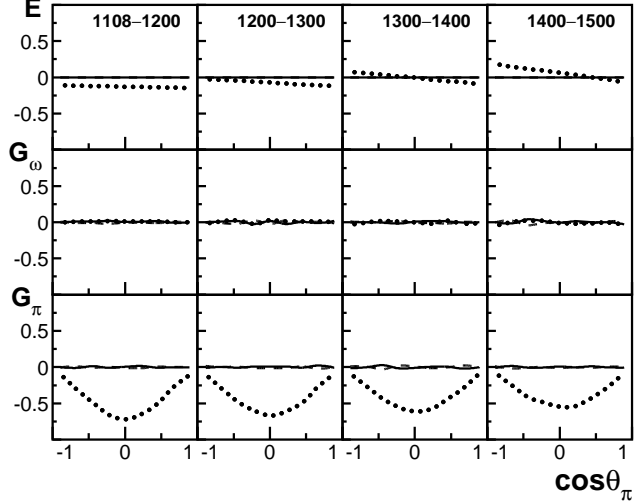


**Fig. 7.** Prediction for the helicity asymmetry  $E$  and the asymmetries  $G$  and  $G_\pi$  as a function of the angle between beam and  $\pi$ -meson calculated in the c.m.s. of the reaction. Notation of curves and energy bins is the same as in Fig. 5.

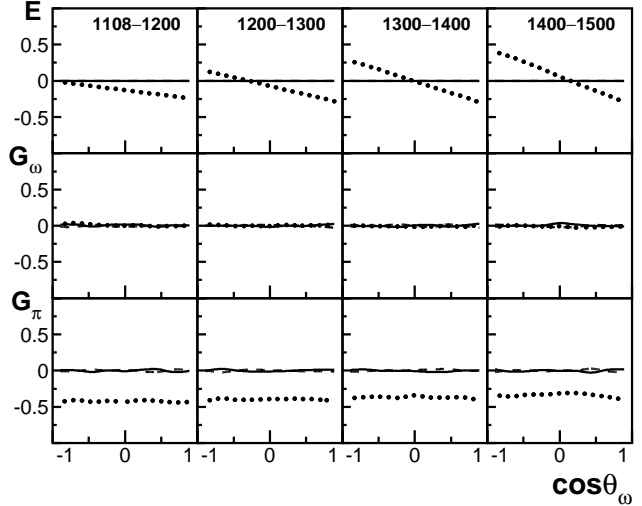


**Fig. 8.** Prediction of the helicity asymmetry  $E$  and the asymmetries  $G$  and  $G_\pi$  as a function of the angle between beam and  $\omega$ -meson calculated in the c.m.s. of the reaction. Notation of curves and energy bins is the same as in Fig. 5.

At small initial energies where the omega momentum is small against its energy ( $|\mathbf{w}| < M_\omega$ ) this yields:

$$\Sigma_\pi^\omega = \frac{1 - z_\pi^{\omega 2}}{1 + z_\pi^{\omega 2}}. \quad (63)$$

Similar to the case of pure  $\pi$ -exchange, this observable does not depend on the  $\omega$ -meson production angle. However the sign of  $\Sigma_\pi^\omega$  changes for Pomeron exchange:

$$\Sigma_\pi^\omega = \frac{1 - 1/3}{1 + 1/3} = \frac{1}{2} \quad (64)$$

Apart from the overall sign, the behavior of the pion asymmetry  $\Sigma_\pi$  is very similar for pure pion and pomeron ex-



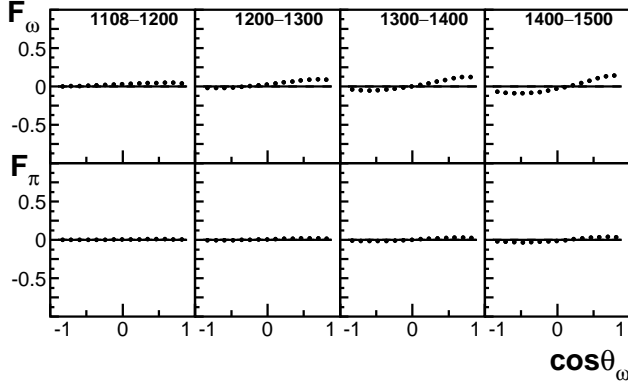


**Fig. 9.** Prediction for the  $F_\omega$  and  $F_\pi$  asymmetries as a function of the angle between beam and  $\omega$ -meson calculated in the c.m.s. of the reaction. Notation of curves and energy bins is the same as in Fig. 5.

change mechanisms. The omega asymmetry  $\Sigma_\omega$  is zero in both cases.

Results of simulations of the omega and pion asymmetries using the Bonn-Gatchina fitting program are shown in Figs. 5 and 6 for pure pomeron exchange. As expected  $\Sigma_\pi$  hardly deviates from the  $(1 - z_\pi^2)/(1 + z_\pi^2)$  in the threshold region and  $\Sigma_\omega$  vanishes.

### 3.3 Mixing of pion and pomeron exchange amplitudes

To fix the mixing between the pion and pomeron amplitudes we fitted the unpolarized differential cross section measured by the SAPHIR collaboration from the  $\omega$  production threshold at 1723 MeV to 2.4 GeV [8]. The fit roughly reproduced the total cross section. The description of the differential cross section was rather limited. The contributions of the two mechanisms to the total cross section was found to be about 40% for pomeron and 60% for pion exchange. The results in the beam asymmetries for such a mixing of the pion and pomeron exchange amplitudes are shown as dotted curves in Figs. 5 and 6. These amplitudes do not interfere if the nucleon is not polarized. Hence, the omega asymmetry is close to zero and the  $\Sigma_\pi$  asymmetry only weakly depends on the angle of the omega meson with respect to the beam.

### 3.4 Double polarization observables

In experiments with polarized beam and polarized target information about further polarization variables can be extracted. Predictions for the angular dependence of  $E$ ,  $G$  and  $G_\pi$  are shown in Figs. 7 and 8 for the cases of pion and/or pomeron exchanges. It can be seen that for pure pion or pomeron exchange all these double polarization asymmetries are equal to zero. In the case of mixing of pomeron and pion exchange amplitudes  $G_\omega$  remains zero. However,  $E$  shows a clear linear dependence of both  $z_\omega$  and  $z_\pi$ . Also  $G_\pi$  exhibits a clear deviation from zero. It

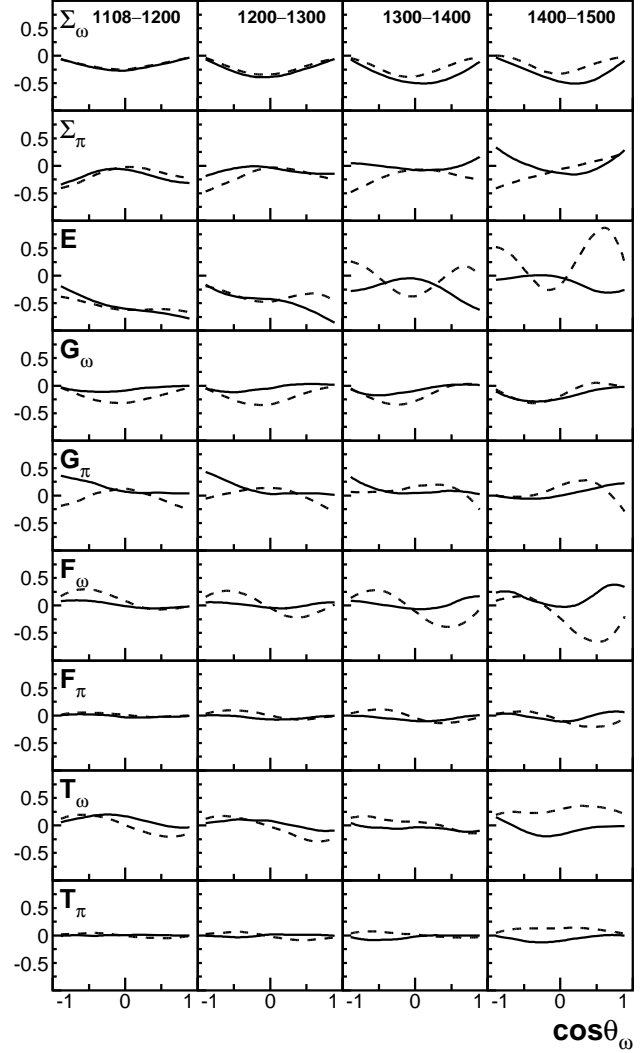


**Fig. 10.** Prediction for the  $\cos \theta_\omega$  dependence of polarization variables for two solutions with dominant contributions from s-channel resonances. The solution 1 shown by solid curve and solution 2 by dashed curves.

depends on  $z_\pi$  like  $-A(1 - z_\pi^2)/(1 + z_\pi^2)$  ( $1 > A > 0$ ) and is approximately flat in  $z_\omega$ .

With transverse target polarization the target asymmetry  $T$  is equal to zero for all three cases. The observables  $F_\omega$ ,  $F_\pi$  can be extracted from measurements with circular polarized beam. As it is shown in Fig. 9 they also remain very small in the case of pion and/or pomeron exchange.

### 3.5 Sensitivity of the polarization variables to contributions from s-channel resonances

Recent experiments [8,10,14] indicated that, in addition to  $\pi^0$  and pomeron exchange, s-channel resonances play a significant role in  $\omega$  photoproduction in the threshold region. Therefore we investigated their impact on the polarization observables for the  $\omega \rightarrow \pi^0 \gamma$  final state using the frame of the Bonn-Gatchina partial wave analysis (PWA)

program. Reasonably good agreement with the data is obtained for several different PWA solutions. Two, labeled (1) and (2), reproduce well the differential cross sections [8] and the omega asymmetry  $\Sigma_\omega$  even though the physical content of both solutions is rather different. In (1) two  $P_{13}$  resonances provide the most significant contributions while (2) is dominated by  $N(1680)F_{15}$ . Further solutions exist and cannot be distinguished on the basis of the available data.

Fig. 10 shows the results for single and double polarization variables of the two solutions (1) and (2). Already data on the pion asymmetry  $\Sigma_\pi$ , which can be extracted from an experiment with linearly polarized beam and unpolarized target, will help to distinguish these two solutions. Very large differences are observed in the helicity asymmetry  $E$  (circularly polarized beam and longitudinally polarized target) and in the observable  $F_\omega$  (circularly polarized beam and transverse target polarization).

## 4 Summary and Conclusions

We have studied single and double polarization observables in the photoproduction of  $\omega$ -mesons with subsequent radiative decay  $\omega \rightarrow \pi^0\gamma$ . It is shown that the pion and pomeron exchange amplitudes have a very specific signature in the omega asymmetry  $\Sigma_\omega$ , the pion asymmetry  $\Sigma_\pi$ , the pion-in-omega-rest-frame asymmetry  $\Sigma_\pi^\omega$  and in the double polarization asymmetry  $G_\pi$ . The measurements of these and further double polarization observables will be very important to distinguish between the t-channel exchange contributions and additional s-channel resonance production. In the Bonn-Gatchina PWA the observables  $E$  and  $G_\pi$  appear particularly sensitive to distinguish between different partial wave solutions which describe the available data on the same level.

## Acknowledgements

We would like to thank Eberhard Klempt and Alexander Titov for useful discussions and remarks. This work was supported by the Deutsche Forschungsgemeinschaft within the SFB/TR16, and the Russian Foundation for Basic Research (07-02-01196-a).

## References

1. N. Isgur, "Baryons: The promise, the problems, and the prospects," *7th International Conference on the Structure of Baryons*, (B.F. Gibson *et al.* eds.), Santa Fe, New Mexico, 3-7 Oct 1995 World Scientific, Singapore, 1996.
2. S. Capstick and N. Isgur, Phys. Rev. D **34** (1986) 2809.  
S. Capstick and W. Roberts, Prog. Part. Nucl. Phys. **45** (2000) S241.
3. L. Y. Glozman, W. Plessas, K. Varga and R. F. Wagenbrunn, Phys. Rev. D **58** (1998) 094030.
4. U. Löring, K. Kretzschmar, B. C. Metsch and H. R. Petry, Eur. Phys. J. A **10** (2001) 309.  
U. Löring, B. C. Metsch and H. R. Petry, Eur. Phys. J. A **10** (2001) 395, 447.
5. Particle Data Group, Phys. Lett. **B592** (2004).
6. N. Isgur and G. Karl, Phys. Lett. **72B** (1977) 109
7. R. Koniuk and N. Isgur, Phys. Rev. D **21** (1980) 1868
8. J. Barth *et al.*, Eur. Phys. J. A **18** (2003) 117.
9. P. Ambrozewicz *et al.*, Phys. Rev. C **70** (2004) 035203
10. J. Ajaka *et al.*, Phys. Rev. Lett. **96** (2006) 132003.
11. G. Penner, U. Mosel, Phys. Rev. C **66** (2002) 055211, 055212
12. Shklyar, H. Lenske, U. Mosel and G. Penner, Phys. Rev. C **71** (2005) 055206;  
*erratum* C **72** (2005) 019903.
13. Q. Zhao, J.S. Al-Khalili, and P.L. Cole, Phys. Rev. C **71** (2005) 054004
14. H. Schmieden, Proceedings of the NSTAR2007 workshop, arXiv:0711.4056[nucl-ex]
15. W. T. Chiang *et al.*, Phys. Rev. C **68** (2003) 045202.  
T. Mart, C. Bennhold, H. Haberzettl and L. Tiator, "KaonMAID 2000" at [www.kph.uni-mainz.de/MAID/kaon/kaonmaid.html](http://www.kph.uni-mainz.de/MAID/kaon/kaonmaid.html).
16. I. S. Barker, A. Donnachie and J. K. Storrow, Nucl. Phys. B **95** (1975) 347.
17. K. Schilling, P. Seyboth and G. E. Wolf, Nucl. Phys. B **15** (1970) 397 [Erratum-ibid. B **18** (1970) 332].
18. Q. Zhao, Phys. Rev. C **63** (2001) 025203 [arXiv:nucl-th/0010038].
19. A.I. Titov and T.-S.H. Lee, Phys. Rev. C **66** (2002) 015204
20. L. Criegee *et al.*, Phys. Rev. Lett. **25**, 1306 (1970).
21. J. Ballam *et al.*, Phys. Rev. D **7** (1973) 3150.
22. J. Ballam *et al.*, Phys. Rev. Lett **24** (1970) 1364; **26** (1971) 155(E).
23. V. Liebenau, Doctoral Thesis, BONN-IR-1983-14.
24. M. Atkinson *et al.*, Nucl. Phys. B **231** (1984) 15.
25. F.J. Gilman *et al.*, Phys. Lett B **31** (1970) 387.
26. B. Friman and M. Soyeur, Nucl. Phys. A **600** (1996) 477.

